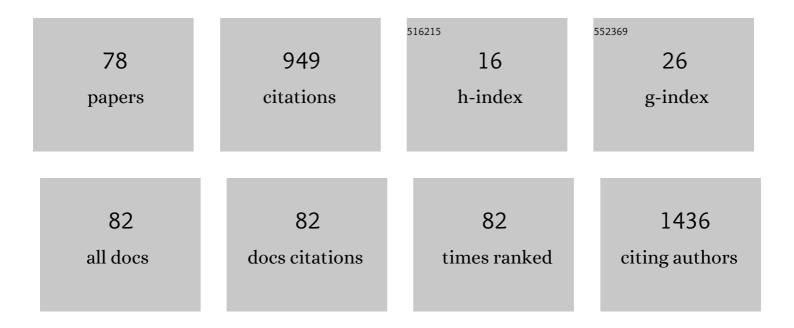
Dr med Dominik Geisel

List of Publications by Year in descending order

Source: https://exaly.com/author-pdf/1123991/publications.pdf Version: 2024-02-01



#	Article	IF	CITATIONS
1	Porcine Liver Decellularization Under Oscillating Pressure Conditions: A Technical Refinement to Improve the Homogeneity of the Decellularization Process. Tissue Engineering - Part C: Methods, 2015, 21, 303-313.	1.1	57
2	ls There Long-term Signal Intensity Increase in the Central Nervous System on T1-weighted Images after MR Imaging with the Hepatospecific Contrast Agent Gadoxetic Acid? A Cross-sectional Study in 91 Patients. Radiology, 2017, 282, 708-716.	3.6	53
3	DNA Double-Strand Breaks after Percutaneous Transluminal Angioplasty. Radiology, 2008, 248, 852-859.	3.6	50
4	Improved rat liver decellularization by arterial perfusion under oscillating pressure conditions. Journal of Tissue Engineering and Regenerative Medicine, 2017, 11, 531-541.	1.3	48
5	CT Body Composition of Sarcopenia and Sarcopenic Obesity: Predictors of Postoperative Complications and Survival in Patients with Locally Advanced Esophageal Adenocarcinoma. Cancers, 2021, 13, 2921.	1.7	38
6	Imaging-based evaluation of liver function: comparison of 99mTc-mebrofenin hepatobiliary scintigraphy and Gd-EOB-DTPA-enhanced MRI. European Radiology, 2015, 25, 1384-1391.	2.3	34
7	Improved Hypertrophy of Future Remnant Liver after Portal Vein Embolization with Plugs, Coils and Particles. CardioVascular and Interventional Radiology, 2014, 37, 1251-1258.	0.9	33
8	Mesenteric Fibrosis in Midgut Neuroendocrine Tumors: Functionality and Radiological Features. Neuroendocrinology, 2018, 106, 139-147.	1.2	33
9	COVID-19 vs. Classical Myocarditis Associated Myocardial Injury Evaluated by Cardiac Magnetic Resonance and Endomyocardial Biopsy. Frontiers in Cardiovascular Medicine, 2021, 8, 737257.	1.1	33
10	DNA double-strand breaks as potential indicators for the biological effects of ionising radiation exposure from cardiac CT and conventional coronary angiography: a randomised, controlled study. European Radiology, 2012, 22, 1641-1650.	2.3	32
11	The catalytically inactive precursor of cathepsin D induces apoptosis in human fibroblasts and HeLa cells. Journal of Cellular Biochemistry, 2007, 101, 1558-1566.	1.2	27
12	Portal vein embolization with plug/coils improves hepatectomy outcome. Journal of Surgical Research, 2015, 194, 202-211.	0.8	27
13	Gd-EOB-DTPA-enhanced MRI for monitoring future liver remnant function after portal vein embolization and extended hemihepatectomy: A prospective trial. European Radiology, 2017, 27, 3080-3087.	2.3	25
14	Cholangiocarcinoma: CT-guided High-Dose Rate Brachytherapy (CT-HDRBT) for Limited (<4 cm) and Large (>4 cm) Tumors. Anticancer Research, 2018, 38, 5843-5852.	0.5	22
15	Predicting liver failure after extended right hepatectomy following right portal vein embolization with gadoxetic acid-enhanced MRI. European Radiology, 2019, 29, 5861-5872.	2.3	22
16	Hepatocellular adenomas: is there additional value in using Gd-EOB-enhanced MRI for subtype differentiation?. European Radiology, 2020, 30, 3497-3506.	2.3	22
17	Increase in left liver lobe function after preoperative right portal vein embolisation assessed with gadolinium-EOB-DTPA MRI. European Radiology, 2013, 23, 2555-2560.	2.3	18
18	Tomoelastography for Measurement of Tumor Volume Related to Tissue Stiffness in Pancreatic Ductal Adenocarcinomas. Investigative Radiology, 2020, 55, 769-774.	3.5	18

#	Article	IF	CITATIONS
19	Factors influencing hypertrophy of the left lateral liver lobe after portal vein embolization. Langenbeck's Archives of Surgery, 2015, 400, 237-246.	0.8	17
20	Treatment for liver metastasis from renal cell carcinoma with computed-tomography-guided high-dose-rate brachytherapy (CT-HDRBT): a case series. World Journal of Urology, 2013, 31, 1525-1530.	1.2	16
21	Hepatopulmonary shunting in patients with primary and secondary liver tumors scheduled for radioembolization. European Journal of Radiology, 2015, 84, 201-207.	1.2	16
22	Gd-EOB enhanced MRI T1-weighted 3D-GRE with and without elevated flip angle modulation for threshold-based liver volume segmentation. Acta Radiologica, 2015, 56, 1419-1427.	0.5	15
23	COVIDâ€∎9â€convalescence phase unmasks a silent myocardial infarction due to coronary plaque rupture. ESC Heart Failure, 2021, 8, 971-973.	1.4	15
24	Treatment of hepatic metastases from gastric or gastroesophageal adenocarcinoma with computed tomography-guided high-dose-rate brachytherapy (CT-HDRBT). Anticancer Research, 2012, 32, 5453-8.	0.5	14
25	Anatomic variants of arteries often coil-occluded prior to hepatic radioembolization. Acta Radiologica, 2015, 56, 159-165.	0.5	12
26	Engineering an endothelialized, endocrine Neo-Pancreas: Evaluation of islet functionality in an ex vivo model. Acta Biomaterialia, 2020, 117, 213-225.	4.1	12
27	Artificial intelligenceâ€based analysis of body composition in Marfan: skeletal muscle density and psoas muscle index predict aortic enlargement. Journal of Cachexia, Sarcopenia and Muscle, 2021, 12, 993-999.	2.9	12
28	HBP-enhancing hepatocellular adenomas and how to discriminate them from FNH in Gd-EOB MRI. BMC Medical Imaging, 2021, 21, 28.	1.4	11
29	No infectious hepatic complications following radioembolization with 90Y microspheres in patients with biliodigestive anastomosis. Anticancer Research, 2014, 34, 4315-21.	0.5	11
30	An increased flip angle in late phase Gd-EOB-DTPA MRI shows improved performance in bile duct visualization compared to T2w-MRCP. European Journal of Radiology, 2014, 83, 1723-1727.	1.2	10
31	Consistency of hepatocellular gadoxetic acid uptake in serial MRI examinations for evaluation of liver function. Abdominal Radiology, 2019, 44, 2759-2768.	1.0	10
32	A radiomics-based model to classify the etiology of liver cirrhosis using gadoxetic acid-enhanced MRI. Scientific Reports, 2021, 11, 10778.	1.6	10
33	Diagnostic Accuracy of Split-Bolus Single-Phase Contrast-Enhanced Cone-Beam CT for the Detection of Liver Tumors before Transarterial Chemoembolization. Journal of Vascular and Interventional Radiology, 2017, 28, 1378-1385.	0.2	9
34	Obesity and pituitary gland volume – a correlation study using three-dimensional magnetic resonance imaging. Neuroradiology Journal, 2020, 33, 400-409.	0.6	9
35	Automatized Hepatic Tumor Volume Analysis of Neuroendocrine Liver Metastases by Gd-EOB MRI—A Deep-Learning Model to Support Multidisciplinary Cancer Conference Decision-Making. Cancers, 2021, 13, 2726.	1.7	9
36	Comparing HCC arterial tumour vascularisation on baseline imaging and after lipiodol cTACE: how do estimations of enhancing tumour volumes differ on contrast-enhanced MR and CT?. European Radiology, 2020, 30, 1601-1608.	2.3	8

Dr med Dominik Geisel

#	Article	IF	CITATIONS
37	Added Value of Tomoelastography for Characterization of Pancreatic Neuroendocrine Tumor Aggressiveness Based on Stiffness. Cancers, 2021, 13, 5185.	1.7	8
38	DNA double-strand breaks in blood lymphocytes induced by two-day 99mTc-MIBI myocardial perfusion scintigraphy. European Radiology, 2018, 28, 3075-3081.	2.3	7
39	Is there a Role for the Appleby Procedure in 2020? Results from a Matched-Pair-Analysis. Anticancer Research, 2020, 40, 387-392.	0.5	7
40	Treatment of a giant hepatic echinococcal cyst with percutaneous drainage and in vivo assessment of the protoscolicidal effect of praziquantel. Clinical Journal of Gastroenterology, 2021, 14, 888-892.	0.4	7
41	First PACSâ€integrated artificial intelligenceâ€based software tool for rapid and fully automatic analysis of body composition from CT in clinical routine. JCSM Clinical Reports, 2022, 7, 3-11.	0.5	7
42	Performance survey on a new standardized formula for oral signal suppression in MRCP. European Journal of Radiology Open, 2018, 5, 1-5.	0.7	6
43	C-Arm Cone Beam CT for Intraprocedural Image Fusion and 3D Guidance in Portal Vein Embolization (PVE). CardioVascular and Interventional Radiology, 2018, 41, 424-432.	0.9	6
44	Feasibility and Safety of CT-Guided High-Dose-Rate Brachytherapy Combined with Transarterial Chemoembolization Using Irinotecan-Loaded Microspheres for the Treatment of Large, Unresectable Colorectal Liver Metastases. Journal of Vascular and Interventional Radiology, 2020, 31, 315-322.	0.2	6
45	Evaluation of gadolinium-EOB-DTPA uptake after portal vein embolization: value of an increased flip angle. Acta Radiologica, 2014, 55, 149-154.	0.5	5
46	Comparison of CT and MRI artefacts from coils and vascular plugs used for portal vein embolization. European Journal of Radiology, 2014, 83, 692-695.	1.2	5
47	Primary and metastatic malignancies of the lung: Retrospective analysis of the CT-guided high-dose rate brachytherapy (CT-HDRBT) ablation in tumours <4 cm and ≥4 cm. European Journal of Radiology 2018, 108, 230-235.	,1.2	5
48	Gd-EOB-DTPA-enhanced MRI T1 relaxometry as an imaging-based liver function test compared with 13C-methacetin breath test. Acta Radiologica, 2020, 61, 291-301.	0.5	5
49	Gadoxetic acid-enhanced MRI in primary sclerosing cholangitis: added value in assessing liver function and monitoring disease progression. Abdominal Radiology, 2021, 46, 979-991.	1.0	5
50	Primary renal sarcomas: imaging features and discrimination from non-sarcoma renal tumors. European Radiology, 2022, 32, 981-989.	2.3	5
51	Influence of Baseline CT Body Composition Parameters on Survival in Patients with Pancreatic Adenocarcinoma. Journal of Clinical Medicine, 2022, 11, 2356.	1.0	5
52	Split-bolus vs. multiphasic contrast bolus protocol in patients with pancreatic cancer or cholangiocarcinoma. European Journal of Radiology, 2019, 119, 108626.	1.2	4
53	Portosystemic shunt surgery in the era of TIPS: imaging-based planning of the surgical approach. Abdominal Radiology, 2020, 45, 2726-2735.	1.0	4
54	CT fluoroscopyâ€guided pancreas transplant biopsies: a retrospective evaluation of predictors of complications and success rates. Transplant International, 2021, 34, 855-864.	0.8	4

Dr med Dominik Geisel

#	Article	IF	CITATIONS
55	Impact of Doppler Ultrasound on Diagnosis and Therapy Control of Lienalis Steal Syndrome After Liver Transplantation. Annals of Transplantation, 2017, 22, 440-445.	0.5	4
56	The Effect of Fat Distribution on the Inflammatory Response of Multiple Trauma Patients—A Retrospective Study. Life, 2021, 11, 1243.	1.1	4
57	Ventilation/perfusion SPECT or SPECT/CT for lung function imaging in patients with pulmonary emphysema?. Annals of Nuclear Medicine, 2015, 29, 528-534.	1.2	3
58	Combined morphological and functional liver MRI using spin-lattice relaxation in the rotating frame (T1Ï) in conjunction with Gadoxetic Acid-enhanced MRI. Scientific Reports, 2019, 9, 2083.	1.6	3
59	Optimized separation of left and right liver lobe in dynamic 99mTc-mebrofenin hepatobiliary scintigraphy using a hybrid SPECT-CT scanner. Annals of Nuclear Medicine, 2014, 28, 897-902.	1.2	2
60	Hepatopulmonary shunting after surgical, interventional and systemic therapy in patients with liver malignancies scheduled for radioembolization. Acta Radiologica, 2016, 57, 908-913.	0.5	2
61	The Magnetic Field of Magnetic Resonance Imaging Systems Does Not Affect Cells Labeled with Micrometer-Sized Iron Oxide Particles. Tissue Engineering - Part C: Methods, 2017, 23, 412-421.	1.1	2
62	Optimized imaging of the lower abdomen and pelvic region in hepatocyte-specific MRI: evaluation of a whole-abdomen first-pass shuttle protocol in patients with neuroendocrine neoplasms. Acta Radiologica, 2019, 60, 1074-1083.	0.5	2
63	Evaluating hepatotoxic effects of chemotherapeutic agents with gadoxetic-acid-enhanced magnetic resonance imaging. European Journal of Radiology, 2020, 124, 108807.	1.2	2
64	Impact of quantitative pulmonary emphysema score on the rate of pneumothorax and chest tube insertion in CT-guided lung biopsies. Scientific Reports, 2020, 10, 10978.	1.6	2
65	Impact of interventionalist's experience and gender on radiation dose and procedural time in CT-guided interventions—a retrospective analysis of 4380 cases over 10 years. European Radiology, 2021, 31, 569-579.	2.3	2
66	Predicting the Risk of Postoperative Complications in Patients Undergoing Minimally Invasive Resection of Primary Liver Tumors. Journal of Clinical Medicine, 2021, 10, 685.	1.0	2
67	Acute left ventricular insufficiency in a Burkitt Lymphoma patient with myocardial involvement and extensive local tumor cell lysis: a case report. BMC Cardiovascular Disorders, 2022, 22, 31.	0.7	2
68	Visibility of Hypovascularized Liver Tumors during Intra-Arterial Therapy Using Split-Bolus Single-Phase Cone Beam CT. CardioVascular and Interventional Radiology, 2019, 42, 260-267.	0.9	1
69	Liver function quantification of patients with portal vein embolization using dynamic contrast-enhanced MRI for assessment of hepatocyte uptake and elimination. Physica Medica, 2020, 76, 207-220.	0.4	1
70	Stent performance in palliative transhepatic treatment of malignant biliary obstruction: a randomized study comparing covered versus uncovered stents. Acta Radiologica, 2020, 61, 1591-1599.	0.5	1
71	The Renal Resistive Index in Allografts: Is Sonographic Assessment Sufficiently Reproducible in a Routine Clinical Setting? – Reproducibility of the Renal Resistive Index. RoFo Fortschritte Auf Dem Gebiet Der Rontgenstrahlen Und Der Bildgebenden Verfahren, 2020, 192, 561-566.	0.7	1
72	Postoperative single-sequence (PoSSe) MRI: imaging work-up for CT-guided or endoscopic drainage indication of collections after hepatopancreaticobiliary surgery. Abdominal Radiology, 2021, 46, 3418-3427.	1.0	1

#	Article	IF	CITATIONS
73	Spectral CT Hybrid Images in the Diagnostic Evaluation of Hypervascular Abdominal Tumors—Potential Advantages in Clinical Routine. Diagnostics, 2021, 11, 1539.	1.3	1
74	Effects of Artificial Intelligence-Derived Body Composition on Kidney Graft and Patient Survival in the Eurotransplant Senior Program. Biomedicines, 2022, 10, 554.	1.4	1
75	The Predictive Value of the Maximal Liver Function Capacity Test for the Isolation of Primary Human Hepatocytes. Tissue Engineering - Part C: Methods, 2018, 24, 179-186.	1.1	Ο
76	Intrahepatic De Novo Tumors in Liver Recipients are Highly Associated With Recurrent Viral Hepatitis. Journal of Clinical and Experimental Hepatology, 2021, 11, 435-442.	0.4	0
77	Giant Gallbladder Empyema in Mirizzi Syndrome. Deutsches Ärzteblatt International, 2019, 116, 300.	0.6	Ο
78	Does Hepatic Steatosis Influence the Detection Rate of Metastases in the Hepatobiliary Phase of Gadoxetic Acid-Enhanced MRI?. Journal of Clinical Medicine, 2021, 10, 98.	1.0	0